Applied Energy 156 (2015) 280–289

Contents lists available at ScienceDirect

Applied Energy

journal homepage: www.elsevier.com/locate/apenergy

Performance analysis of a dual-loop organic Rankine cycle (ORC) system with wet steam expansion for engine waste heat recovery

Jian Song *, Chun-wei Gu

Key Laboratory for Thermal Science and Power Engineering of Ministry of Education, Department of Thermal Engineering, Tsinghua University, Beijing 100084, China

HIGHLIGHTS

- A dual-loop ORC system is designed for engine waste heat recovery.
- Wet steam expansion of water is applied in the HT loop.
- The influence of the HT loop operating conditions on the LT loop is evaluated.
- Pinch point locations determine the thermal parameters of the LT loop.

ARTICLE INFO

Article history:
Received 24 April 2015
Received in revised form 12 June 2015
Accepted 12 July 2015
Available online 24 July 2015

Keywords:
ORC
Dual-loop system
Wet steam expansion
Engine waste heat recovery

ABSTRACT

A dual-loop organic Rankine cycle (ORC) system is designed to recover the waste heat of a diesel engine. The high-temperature (HT) loop utilizes the heat load of the engine exhaust gas, and the low-temperature (LT) loop uses the heat load of the jacket cooling water and the residual heat of the HT loop sequentially. These two loops are coupled via a shared heat exchanger. Water is selected as the working fluid for the HT loop and wet steam expansion, which can be implemented through screw expanders, is exploited. The dryness fraction of the wet steam at the inlet of the expander can be adjusted to attain a suitable evaporation temperature and provide a better temperature match with the heat source. The working fluid candidates for the LT loop are chosen to be R123, R236fa and R245fa. The influence of the HT loop parameters on the performance of the LT loop is evaluated. The simulation results reveal that under different operating conditions of the HT loop, the pinch point of the LT loop occurs at different locations and therefore, results in different evaporation temperatures and other thermal parameters. The maximum net power output of the dual-loop ORC system reaches 115.1 kW, which leads to an increase of 11.6% on the original power output of the diesel engine.

1. Introduction

The diesel engine is a primary power source for automobiles, ships and locomotives mainly due to its robust thermal performance and high operational reliability. In recent decades, the energy consumption of diesel engines has increased rapidly with the development of the transportation industry. However, the global greenhouse effect and the depleted energy supply are crucial issues that the developing world has to face. Governments of many countries have introduced strict regulations for diesel engine emissions and fuel economy standards. Therefore, there is a strong motivation in the propulsion sector to increase the efficiency of diesel engines.

In a typical diesel engine, less than 45% of the fuel energy is converted into a useful power output by the crankshaft, while the remaining energy is lost through the engine exhaust gas, the jacket cooling water, the air cooling system and the lubrication system [1]. It is apparent that a large fraction of the primary energy remains untapped and the potential gain from efficiently recovering the waste heat is appreciable.

The current energy scenario has revived strong interest in the waste heat recovery of diesel engines, which is similar to what occurred in the 1970s in the United States [2] and Europe [3] as a consequence of the first oil crisis. Among all of the existing technologies, the organic Rankine cycle (ORC) has been proven to be a promising solution for engine waste heat recovery [4–11]. Different ORC systems (such as simple ORC systems [12,13], regenerative ORC systems [13,14] and preheated ORC systems [15,16]) have been designed and presented to recover engine waste heat. In addition, dual-loop ORC systems have been actively researched

* Corresponding author. Tel.: +86 10 6278 1739; fax: +86 10 6277 1209.
E-mail address: song-j13@mails.tsinghua.edu.cn (J. Song).

http://dx.doi.org/10.1016/j.apenergy.2015.07.019
0306-2619/

Nomenclature

$\dot{m}$	mass flow rate, kg/s
Q	heat load, kW
h	specific enthalpy, kJ/kg
c_p	specific heat capacity, kJ/kg K
T	temperature, K
W	power, kW
$\dot{I}$	exergy destruction rate, kW
E	exergy
x	dryness fraction

Greek symbols

η	efficiency

Subscripts

wf	working fluid
HT	high-temperature
LT	low-temperature
gas	engine exhaust gas
jw	jacket cooling water
in	inlet
out	outlet
pump	pump
evap	evaporator
exp	expander
cond	condenser
res	residual
c	cooling water
net	net
the	thermal
tot	total
ex	exergy

Acronyms

ORC	organic Rankine cycle
HT	high-temperature
LT	low-temperature
GWP	global warming potential
ODP	ozone depletion potential

in recent years, which can simultaneously recover the waste heat of the engine exhaust gas and the engine coolant. Shu et al. [17] proposed a novel dual-loop organic Rankine cycle system for engine waste heat recovery, which consisted of a high-temperature (HT) loop and a low-temperature (LT) loop. The HT loop used water as the working fluid to recover the high-temperature engine exhaust, and the LT loop used an organic working fluid to sequentially recover the waste heat of the engine coolant, the residual heat of the HT loop and the low-temperature exhaust. Energetic and exergetic analysis were conducted, and the simulation results revealed that the maximum net power output and the maximum exergy efficiency of the system reached 36.77 kW and 55.05%, respectively. Choi and Kim [18] applied a dual-loop waste heat recovery power generation system, which was comprised of an upper trilateral cycle that uses water and a lower organic Rankine cycle, to an internal combustion engine. The HT loop recovered the waste heat of the engine exhaust gas and the LT loop recovered the low-temperature exhaust and the residual heat of the HT loop. The thermodynamic results confirmed that the dual loop system exhibited a maximum net power output of 2069.8 kW, a maximum thermal efficiency of 10.93% (in accordance with the first law of thermodynamics) and a maximum exergy efficiency of 58.77% (in accordance with the second law of thermodynamics). Zhang et al. [19] analyzed the characteristics of a novel system that combined a vehicular light-duty diesel engine with a dual-loop ORC system. A high-temperature loop recovered the exhaust heat, and a low-temperature loop recovered the residual heat from the high-temperature loop and the waste heat from both the intake air and the engine coolant. The relative power output improved from 14% to 16% in the peak effective thermal efficiency region of the engine and from 38% to 43% in the small load region. Panesar et al. [20] presented a dual loop ORC system for long haul trucks. A water blend study was conducted to identify suitable mixtures for the high-temperature loop, while the low-temperature loop used a hydrofluoroether fluid as the working fluid. The results showed that the use of the blend in a dual-loop system could increase the engine brake power by 5.8–7.4%.

Though water has been selected to be the working fluid in the HT loop for dual-loop ORC systems, few studies have considered exploiting wet steam expansion, which can be implemented through screw expanders. Moreover, for most current dual-loop ORC systems, the LT loop utilized the low-temperature waste heat in addition to the residual heat of the HT loop. It is evident that the residual heat load of the HT loop varies under different operating conditions, and this has an impact on the LT loop. However, few studies have concentrated on the influence of the HT loop parameters on the LT loop. In this paper, these two issues (i.e., the exploitation of wet steam expansion and the influence of the HT loop parameters on the LT loop) have been investigated. A dual-loop ORC system is designed to recover the waste heat of a diesel engine manufactured by Hudong Heavy Machinery Co., Ltd. In this system, the HT loop utilizes the heat load of the engine exhaust gas, while the LT loop recovers the heat load of the jacket cooling water and the residual heat of the HT loop. The two loops of this system are coupled via a shared heat exchanger. Wet steam expansion with water as the working fluid is exploited in the HT loop, and R123, R236fa and R245fa are chosen as the working fluid candidates for the LT loop. Performance analysis is conducted for the dual-loop ORC system with different working fluids and under different operating conditions. The influence of the HT loop parameters on the LT loop is evaluated. The maximum net power output and the maximum exergy efficiency are the evaluation criteria to select the suitable working fluid and define the optimal thermal parameters of the system.

2. System description

2.1. Diesel engine

The selected diesel engine in this paper is an inline six-cylinder turbocharged engine manufactured by Hudong Heavy Machinery

Table 1
Main parameters of the diesel engine.

Property	Unit	Value
Power output	kW	996
Rotation speed	r/min	1500
Torque	N m	6340
Temperature of the engine exhaust gas	K	573.15
Mass flow rate of the engine exhaust gas	kg/h	7139
Inlet temperature of the jacket cooling water	K	338.15
Outlet temperature of the jacket cooling water	K	363.15
Mass flow rate of the jacket cooling water	kg/h	6876

Table 2
Composition of the engine exhaust gas.

Composition	Content (g/kW h)	Molecular weight (g/mol)	Fraction (%)
O_2	1366	32.00	14.83
CO_2	552	44.00	4.36
H_2O	321	18.01	6.20
CO	0.28	28.01	–
SO_2	0.46	64.06	–
NO_x (NO_2)	11.17	46.01	–
HC (CH_4)	0.19	16.04	–
N_2	6872	28.01	74.61

Co., Ltd. The main parameters of the diesel engine are shown in Table 1. The composition of the engine exhaust gas is measured and listed in Table 2. According to a calculation by REFPROP 9.1, the specific heat capacity of the engine exhaust gas is approximately 1.1 kJ/kg K. The heat load will be nearly 600 kW if the engine exhaust gas is cooled to the ambient temperature, and the heat load of the jacket cooling water is 199.9 kW. The total heat load of the two waste heat sources of the diesel engine reaches nearly 800 kW, which further confirms that the efficient recovery of the waste heat will significantly improve the engine power output as well as increase the thermal efficiency without additional fuel consumption.

2.2. Dual-loop ORC system

The schematic diagram of the dual-loop ORC system is shown in Fig. 1. The HT loop recovers the heat load of the engine exhaust gas, while the LT loop utilizes the heat load of the jacket cooling water and the residual heat of the HT loop sequentially. The two loops of the system are coupled via a shared heat exchanger and therefore, the condenser of the HT loop is also the evaporator of the LT loop. By using a shared heat exchanger, the heat load that dissipated to the environment can be significantly reduced, and this reduction increases the overall efficiency and the total power output of the system.

Water is selected to be the working fluid in the HT loop. Because water has the largest latent heat of any known working fluid, a large part of the absorbed heat load is required for evaporation. However, the temperature of the waste heat source decreases continuously as it transfers the heat load to the water. Consequently, the evaporation temperature of the water will be much lower than the initial temperature of the waste heat source, and this results in poor cycle efficiencies. One viable solution is to apply wet steam expansion to the HT loop by means of a screw expander, as an alternative to traditional organic expanders [21]. Screw expanders can operate normally even when the working fluid is wet at the inlet because they enhance the lubrication of the meshing rotors due to the presence of the liquid, which seals the gaps between the rotors and the casing [22]. Moreover, screw expanders are capable of higher rotational speeds than vane and scroll expanders, and the optimal tip speed is approximately one order of magnitude less than that of traditional turbo machines [23]. Therefore, in most cases, screw expanders can be coupled directly to a generator without an intermediate reduction gearbox. This not only reduces the transmission loss but also reduces the capital cost of the system.

In the HT loop, the water from the condenser is first pumped to a high pressure state. Then, in the evaporator, the water absorbs the heat load of the engine exhaust gas and is converted into a two-phase mixture consisting of saturated liquid and saturated vapor. Note that the dryness fraction here can be adjusted to attain a suitable evaporation temperature and provide a better temperature match with the engine exhaust gas. Next, wet steam expansion occurs in the screw expander to produce power, which is later converted into electricity by a generator. Afterward, the two-phase mixture from the expander is condensed into the saturated liquid state.

For the LT loop, R123, R236fa and R245fa are selected to be the working fluid candidates. The properties of these organic fluids are listed in Table 3. Similar to the thermal process of the HT loop, the organic fluid from the condenser is first pumped. Then, it is heated sequentially by the jacket cooling water and the residual heat of the HT loop into the saturated vapor state. It should be emphasized that the evaporation of the working fluid might occur in either heat exchanger and mainly depends on the heat load capacities of the two heat sources. Next, the organic vapor expands in the expander and then, it is condensed by the cooling water in the condenser.

3. Thermodynamic model

The T–s diagram of the dual-loop ORC system with wet steam expansion is shown in Fig. 2. The thermodynamic model of the system is described below.

3.1. HT loop

In the HT loop, the mass flow rate of the water can be calculated using the following equation

$$\dot{m}_{wf,HT} = \frac{Q_{gas}}{h_{4,HT} - h_{2,HT}} \tag{1}$$

where Q_{gas} is the heat load of the engine exhaust gas, which can be calculated as

$$Q_{gas} = \dot{m}_{gas} \cdot c_{p,gas} \cdot (T_{gas,in} - T_{gas,out}) \tag{2}$$

where $c_{p,gas}$ is the average specific heat capacity of the engine exhaust gas, and $T_{gas,in}$ and $T_{gas,out}$ are defined as the inlet and outlet temperatures of the engine exhaust gas, respectively.

Process in the working fluid pump is given by

$$W_{pump,HT} = \frac{\dot{m}_{wf,HT} \cdot (h_{2s,HT} - h_{1,HT})}{\eta_{pump,HT}} \tag{3}$$

$$\dot{I}_{pump,HT} = T_0 \cdot \dot{m}_{wf,HT} \cdot (s_{2,HT} - s_{1,HT}) \tag{4}$$

Process in the evaporator is given by

$$Q_{evap,HT} = \dot{m}_{wf,HT} \cdot (h_{4,HT} - h_{2,HT}) \tag{5}$$

$$h_{4,HT} = (1 - x) \cdot h_{3,HT} + x \cdot h_{4',HT} \tag{6}$$

$$\dot{I}_{evap,HT} = T_0 \cdot \dot{m}_{wf,HT} \cdot (s_{4,HT} - s_{2,HT}) + T_0 \cdot \dot{m}_{gas} \cdot (s_{gas,out} - s_{gas,in}) \tag{7}$$

where $h_{4',HT}$ is the enthalpy of the saturated vapor corresponding to state point 4 of the HT loop, and x is the dryness factor of the wet steam at the outlet of the evaporator as well as that at the inlet of the screw expander.

Process in the screw expander is given by

$$W_{exp,HT} = \dot{m}_{wf,HT} \cdot (h_{4,HT} - h_{5s,HT}) \cdot \eta_{exp,HT} \tag{8}$$

$$\dot{I}_{exp,HT} = T_0 \cdot \dot{m}_{wf,HT} \cdot (s_{5,HT} - s_{4,HT}) \tag{9}$$

The residual heat of the HT loop is given by

$$Q_{res} = m_{wf,HT} \cdot (h_{5,HT} - h_{1,HT}) \tag{10}$$

The net power output of the HT loop is given by

$$W_{net,HT} = W_{exp,HT} - W_{pump,HT} \tag{11}$$

The thermal efficiency of the HT loop is given by

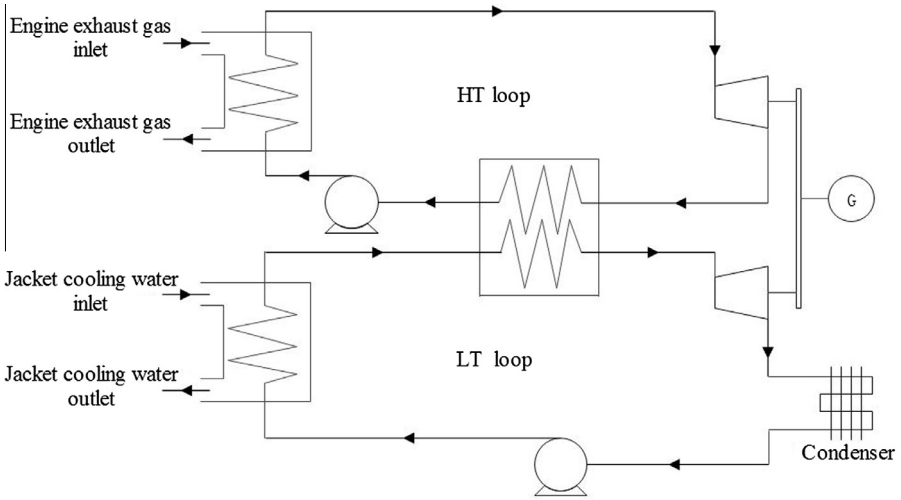

Fig. 1. Schematic diagram of the dual-loop ORC system for engine waste heat recovery.

Table 3
Properties of the working fluids.

Working fluid	Molecular weight (g/mol)	Normal boiling point (K)	Critical temperature (K)	Critical pressure (kPa)	GWP	ODP
R123	152.93	301.0	456.8	3661.8	120	0.012
R236fa	152.04	271.7	398.1	3200.0	9400	0
R245fa	134.05	288.3	427.2	3651.0	950	0

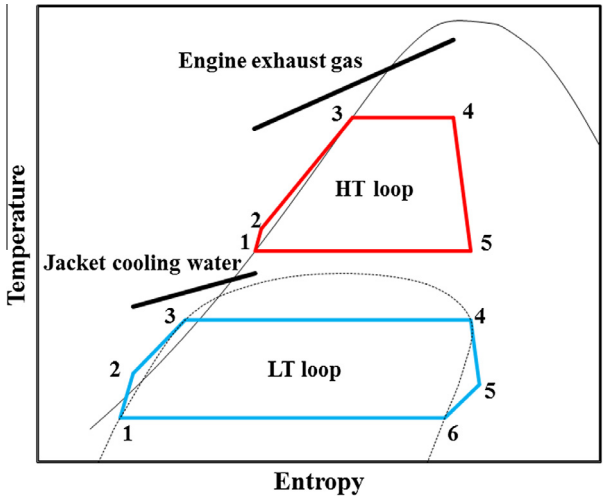

Fig. 2. T–s diagrams of the dual-loop ORC system with wet steam expansion.

$$\eta_{the,HT} = \frac{W_{net,HT}}{Q_{gas}} = \frac{W_{exp,HT} - W_{pump,HT}}{\dot{m}_{gas} \cdot c_{p,gas} \cdot (T_{gas,in} - T_{gas,out})} \tag{12}$$

3.2. LT loop

In the LT loop, the mass flow rate of the working fluid can be calculated using the following equation

$$\dot{m}_{wf,LT} = \frac{Q_{LT}}{h_{4,LT} - h_{2,LT}} = \frac{Q_{jw} + Q_{res}}{h_{4,LT} - h_{2,LT}} \tag{13}$$

where Q_{jw} is the heat load of the exhaust gas, which can be calculated as

$$Q_{jw} = \dot{m}_{jw} \cdot c_{p,jw} \cdot (T_{jw,in} - T_{jw,out}) \tag{14}$$

where $c_{p,jw}$ is the average specific heat capacity of the jacket cooling water, and $T_{jw,in}$ and $T_{jw,out}$ are defined as the inlet and outlet temperatures of the jacket cooling water, respectively.

Process in the working fluid pump is given by

$$W_{pump,LT} = \frac{\dot{m}_{wf,LT} \cdot (h_{2s,LT} - h_{1,LT})}{\eta_{pump,LT}} \tag{15}$$

$$\dot{I}_{pump,LT} = T_0 \cdot \dot{m}_{wf,LT} \cdot (s_{2,LT} - s_{1,LT}) \tag{16}$$

Process in the evaporator (including the two heat exchangers) is given by

$$Q_{evap,LT} = \dot{m}_{wf,LT} \cdot (h_{4,LT} - h_{2,LT}) \tag{17}$$

$$\dot{I}_{evap,LT} = T_0 \cdot \dot{m}_{wf,LT} \cdot (s_{4,LT} - s_{2,LT}) + T_0 \cdot \dot{m}_{wf,HT} \cdot (s_{1,HT} - s_{5,HT}) + T_0 \cdot \dot{m}_{jw} \cdot (s_{jw,out} - s_{jw,in}) \tag{18}$$

Process in the organic expander is given by

$$W_{exp,LT} = \dot{m}_{wf,LT} \cdot (h_{4,LT} - h_{5s,LT}) \cdot \eta_{exp,LT} \tag{19}$$

$$\dot{I}_{exp,LT} = T_0 \cdot \dot{m}_{wf,LT} \cdot (s_{5,LT} - s_{4,LT}) \tag{20}$$

Process in the condenser is given by

$$\dot{m}_{wf,LT} \cdot (h_{5,LT} - h_{1,LT}) = \dot{m}_c \cdot c_{p,c} \cdot (T_{c,out} - T_{c,in}) \tag{21}$$

$$\dot{I}_{cond,LT} = T_0 \cdot \dot{m}_{wf,LT} \cdot (s_{1,LT} - s_{6,LT}) + T_0 \cdot \dot{m}_c \cdot (s_{c,out} - s_{c,in}) \tag{22}$$

where $c_{p,c}$ is the average specific heat capacity of the cooling water and $T_{c,in}$ and $T_{c,out}$ are the inlet and outlet temperatures of the cooling water, respectively.

The net power output of the LT loop is given by

$$W_{net,LT} = W_{exp,LT} - W_{pump,LT} \tag{23}$$

The thermal efficiency of the LT loop can be calculated via

$$\eta_{the,LT} = \frac{W_{net,LT}}{Q_{jw} + Q_{res}} = \frac{W_{exp,LT} - W_{pump,LT}}{Q_{jw} + Q_{res}} \tag{24}$$

3.3. Dual-loop system

The total net power output of the dual-loop system is given by

$$W_{net,tot} = W_{net,HT} + W_{net,LT} \tag{25}$$

The thermal efficiency and the exergy efficiency of the dual-loop system can be calculated via the following equations

$$\eta_{the,tot} = \frac{W_{net,tot}}{Q_{tot}} = \frac{W_{exp,HT} - W_{pump,HT} + W_{exp,LT} - W_{pump,LT}}{Q_{gas} + Q_{jw}} \tag{26}$$

$$\eta_{ex,tot} = \frac{W_{exp,HT} - W_{pump,HT} + W_{exp,LT} - W_{pump,LT}}{\left[\dot{m}_{gas} \cdot c_{p,gas} \cdot (T_{gas,in} - T_0) - T_0 \cdot \ln\frac{T_{gas,in}}{T_0}\right] + \left[\dot{m}_{jw} \cdot c_{p,jw} \cdot (T_{jw,in} - T_{jw,out}) - T_0 \cdot \ln\frac{T_{jw,in}}{T_{jw,out}}\right]} \tag{27}$$

3.4. Conditions and assumptions

The simulation of the dual-loop ORC system in this paper is performed in the FORTRAN environment by a computer program written by the authors. Several conditions and assumptions are given as follows:

(1) the temperature of the cooled exhaust gas is set to be above 378.15 K [24] to avoid acid corrosion;
(2) the heat loss and the pressure loss of the pipelines in the ORC system are ignored;
(3) the efficiencies of the working fluid pump in both loops are set to be 0.8;
(4) the efficiencies of the screw expander and the organic expander are set to be 0.8;
(5) the pinch point temperature differences of the evaporator and the condenser in both loops are set to be 6 K;
(6) the condensation temperatures of the HT loop with water as the working fluid is fixed at 375 K to keep the condensation pressure slightly higher than the atmospheric pressure;
(7) the condensation temperature of the LT loop is fixed at 308.15 K for each working fluid.

4. Results and discussion

4.1. Performance analysis of the HT loop

Because the outlet temperature of the exhaust gas, $T_{gas,out}$, is not fixed, the total heat load absorbed by the HT loop varies. For each specified $T_{gas,out}$, a proper evaporation temperature of the HT loop ($T_{evap,HT} = T_{3,HT} = T_{4,HT}$, see Fig. 2) can be calculated by the computer program, and this temperature is mainly related to the ratio of the latent heat to the sensible heat of the water. Simulations are conducted for the HT loop with water as the working fluid under different operating conditions.

Fig. 3a shows the variation of the outlet temperature of the engine exhaust gas in relation to the dryness fraction of the wet steam under different evaporation temperature conditions. For a specified evaporation temperature of the water, $T_{gas,out}$ increases with the dryness fraction, x. The total heat load absorbed by the HT loop decreases when $T_{gas,out}$ increases, while the heat load required by per unit mass of the wet steam (mainly the latent heat) increases significantly when the dryness fraction increases. Therefore, the mass flow rate of the wet steam decreases when x increases for each evaporation temperature, as shown in Fig. 3b. Fig. 3c illustrates that for each evaporation temperature, the net power output of the HT loop decreases when x increases. This is mainly due to the effect of the decreasing mass flow rate of the wet steam. Fig. 3d shows the variation of the thermal efficiency of the HT loop. A higher evaporation temperature and a higher dryness fraction result in a higher thermal efficiency. Fig. 3e shows that the residual heat load of the HT loop decreases when x increases, because the total heat load absorbed by the LT loop decreases significantly.

The wet steam expansion exhibits better thermal performance for lower dryness fractions. In addition, the residual heat load is larger and can be utilized by the LT loop. Therefore, the dryness fraction of the wet steam entering the screw expander is fixed at 0.2 for the HT loop in this dual-loop ORC system. Fig. 4 shows that with increasing evaporation temperatures, the total heat load absorbed by the HT loop decreases. The net power output of the HT loop decreases as $T_{evap,HT}$ increases and this is due to the effect of the decreasing mass flow rate of the wet steam. The maximum net power output of the HT loop reaches 54.5 kW. The residual heat load of the HT loop is the remaining portion of the total absorbed heat load, and it decreases continuously when $T_{evap,HT}$ increases.

4.2. Performance analysis of the LT loop

R123, R236fa and R245fa are selected as the working fluid candidates for the LT loop. Simulations are conducted under different conditions of the HT loop to evaluate the influence of the HT loop parameters on the LT loop.

Fig. 5a shows the variation of the evaporation temperature of the LT loop. The evaporation temperature of each working fluid decreases when the evaporation temperature of the HT loop increases, because the residual heat load decreases. The variations for R123 and R245fa are similar, whereas the variation for R236fa is remarkably different. When $T_{evap,HT}$ is lower than 490 K, $T_{evap,LT}$ remains constant at 369 K, which is just 6 K (i.e., the pinch point temperature difference) lower than the condensation temperature of the HT loop; when $T_{evap,HT}$ is higher than 490 K and lower than 500 K, $T_{evap,LT}$ decreases significantly when $T_{evap,HT}$ increases; when $T_{evap,HT}$ is higher than 500 K, $T_{evap,LT}$ decreases by a slightly larger amount.

The reason for this phenomenon can be described as follows. The LT loop utilizes the heat load of the jacket cooling water and the residual heat of the HT loop sequentially. The former heat load is kept constant but the residual heat load varies under different operating conditions of the HT loop, which influences the evaporation temperature of the working fluid in the LT loop. The evaporation temperature of a cycle determines the ratio of the latent heat to the sensible heat of the working fluid. Taking the pinch point temperature difference into consideration, the heat load for a heat source above $T_{evap} + \Delta T_{evap}$ is used for evaporation, while the heat load below this temperature is used for preheating the working fluid. As shown in Fig. 6, three cases are presented to comprehensively illustrate the variations of $T_{evap,LT}$ caused by different conditions of the two heat sources. Because the pinch point of the LT loop evaporator appears at different locations, the evaporation temperatures are quite different.

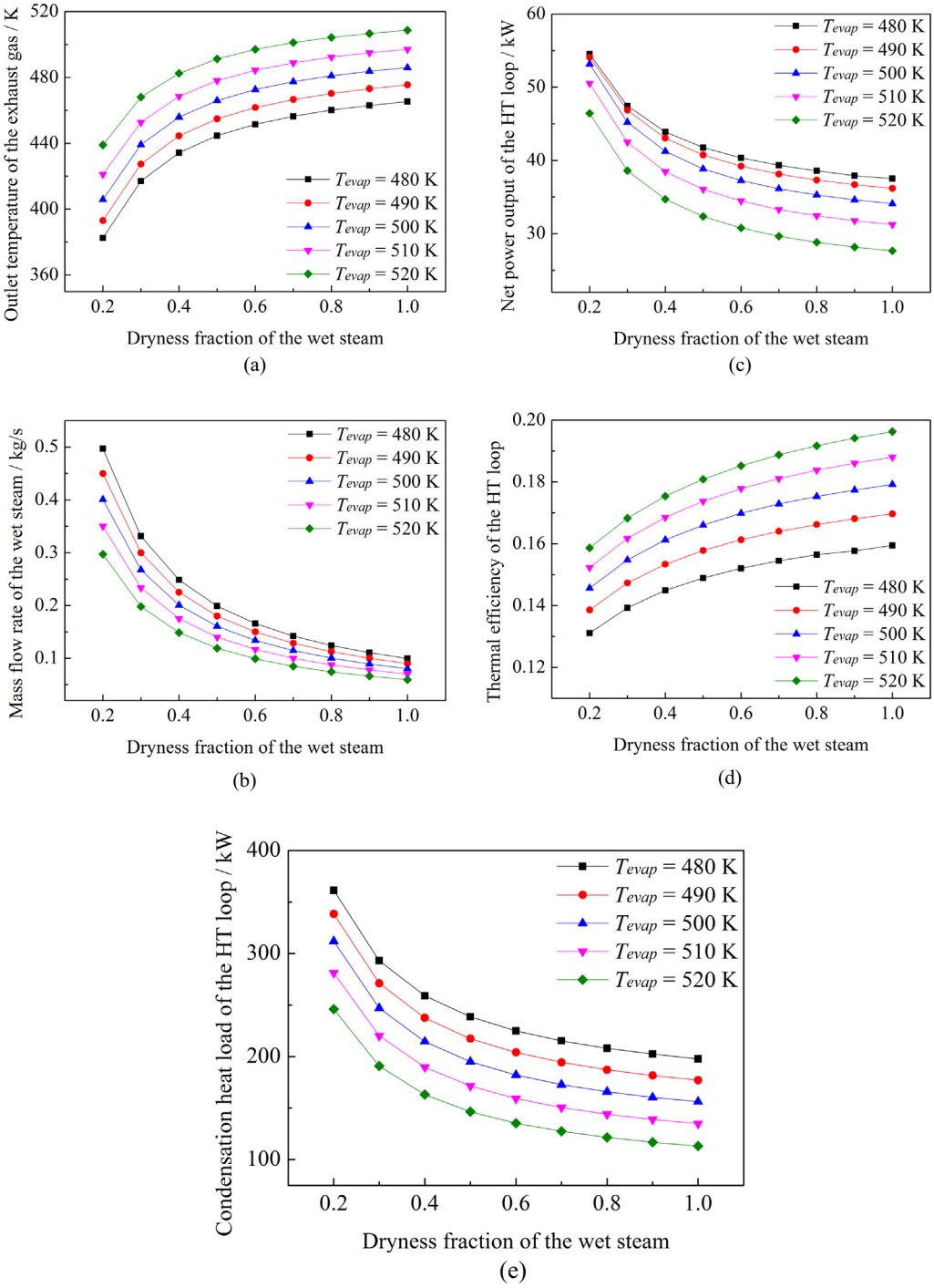

Fig. 3. Variations of the thermal parameters of the HT loop.

If the pinch point appears at the residual heat cycle (see Fig. 6a), a constant evaporation temperature of the LT loop will be attained, which is 6 K (i.e., the pinch point temperature difference) lower than the condensation temperature of the HT loop. This case corresponds to when $T_{evap,LT}$ equals 369 K and $T_{evap,HT}$ is lower than 490 K. If the pinch point appears at the outlet of the jacket cooling water cycle (see Fig. 6b), $T_{evap,LT}$ will be between 357.15 K and 369 K. This case corresponds to when $T_{evap,LT}$ decreases significantly and indicates that $T_{evap,LT}$ is sensitive to the residual heat load of the HT loop. If the pinch point appears at the jacket cooling water cycle (see Fig. 6c), $T_{evap,LT}$ will be lower than 357.15 K. This case corresponds to when $T_{evap,LT}$ decreases slightly and $T_{evap,HT}$ is higher than 500 K.

Fig. 5b demonstrates that the mass flow rates of the working fluids decrease when the evaporation temperature of the HT loop increases, and this is mainly due to the effect of the decreasing residual heat load of the HT loop. The mass flow rate of R236fa is the highest, while that of R123 is the lowest. In Fig. 5c, the net power output of the LT loop decreases continuously as $T_{evap,HT}$ increases, and this is due to both of the effects of the

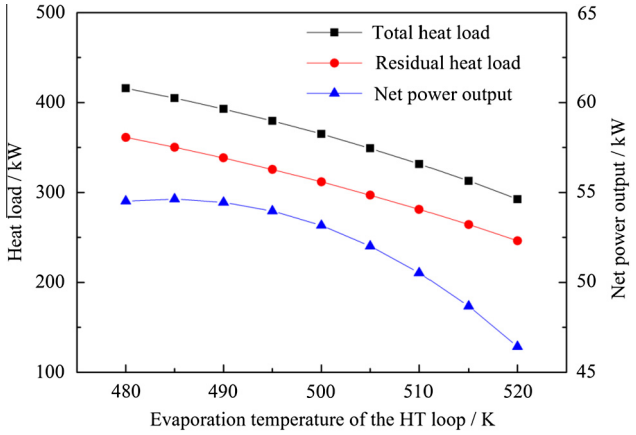

Fig. 4. Variations of the heat loads of the HT loop with wet steam ($x = 0.2$).

decreasing evaporation temperature and the decreasing mass flow rate of the LT loop. The variation of the net power output of R236fa can be divided into three different stages, which is similar to its evaporation temperature. The maximum net power output of the LT loop reaches 60.6 kW with R236fa as the working fluid when $T_{evap,HT}$ equals 480 K. Fig. 5d shows the variation of the thermal efficiency of the LT loop, which confirms that the thermal efficiency is primarily related to the evaporation temperature of the cycle.

4.3. Thermodynamic analysis of the dual-loop ORC system

The total net power outputs of the dual-loop ORC system with different types of working fluids are shown in Fig. 7. Because the net power output of both the HT loop and the LT loop decrease as $T_{evap,HT}$ increases, the total net power output definitely will decrease as well. The variations of the total net power output of R123 and R245fa are similar, while that of R236fa is different, which is mainly influenced by the net power output of the LT loop. The exergy efficiency of the dual-loop ORC system is shown in Fig. 8. The variations of the exergy efficiency of different working fluids are similar to those of the net power output. The maximum exergy efficiency of the dual-loop ORC system reaches 20.6%, with R236fa as the working fluid for the LT loop.

The detailed parameters of the systems with different working fluids are listed in Table 4. When $T_{evap,HT}$ equals 480 K, the HT loop yields the maximum net power output as well as the maximum residual heat load and improves the performance of the LT loop. The evaporation temperature of the LT loop with R236fa is the highest that can be reached and results in a high thermal efficiency. The LT loop with R236fa exhibits a net power output of 60.6 kW, nearly 31.7% and 22.7% higher than those with R123 and R245fa, respectively. According to the simulation results, with wet steam ($x = 0.2$) as the working fluid of the HT loop and R236fa for the LT loop, the total net power output reaches 115.1 kW, which can lead to an increase of 11.6% on the original engine power output.

The exergy analysis of the dual-loop ORC system with wet steam ($x = 0.2$) and R236fa as the working fluids is conducted

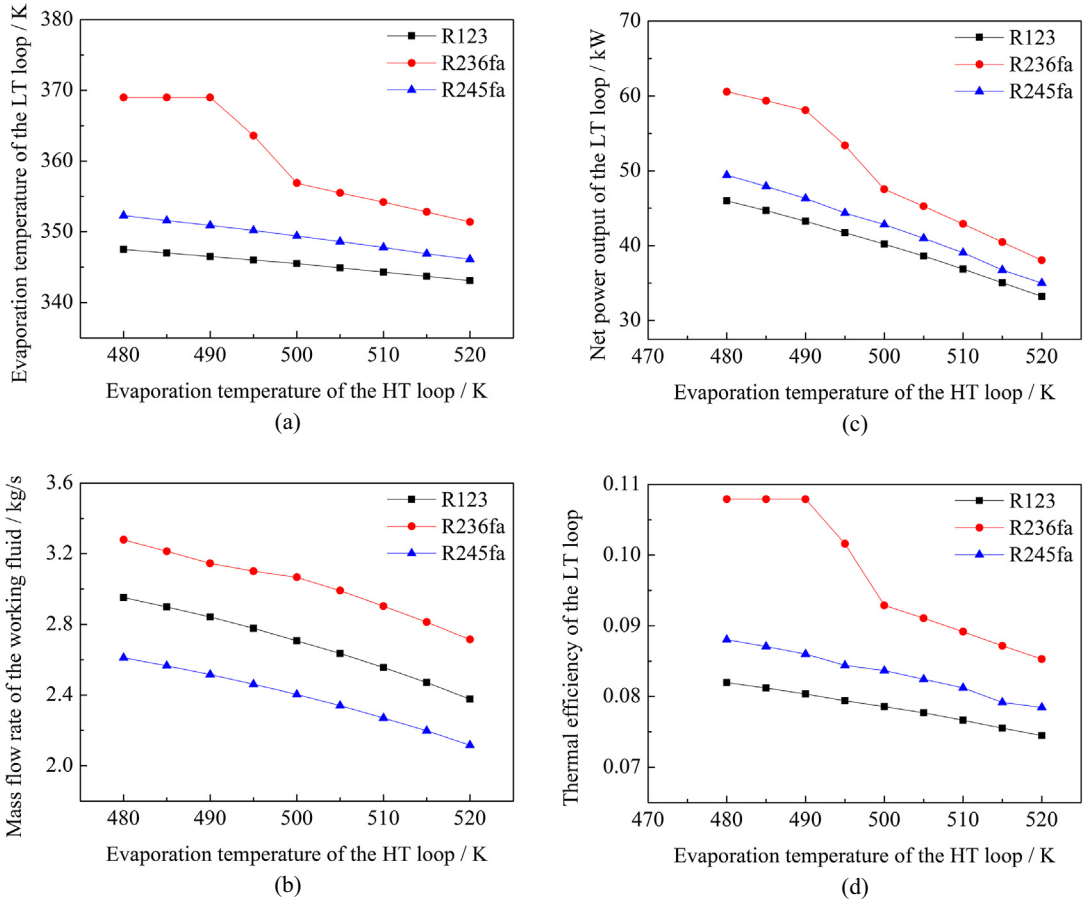

Fig. 5. Variations of the thermal parameters of the LT loop.

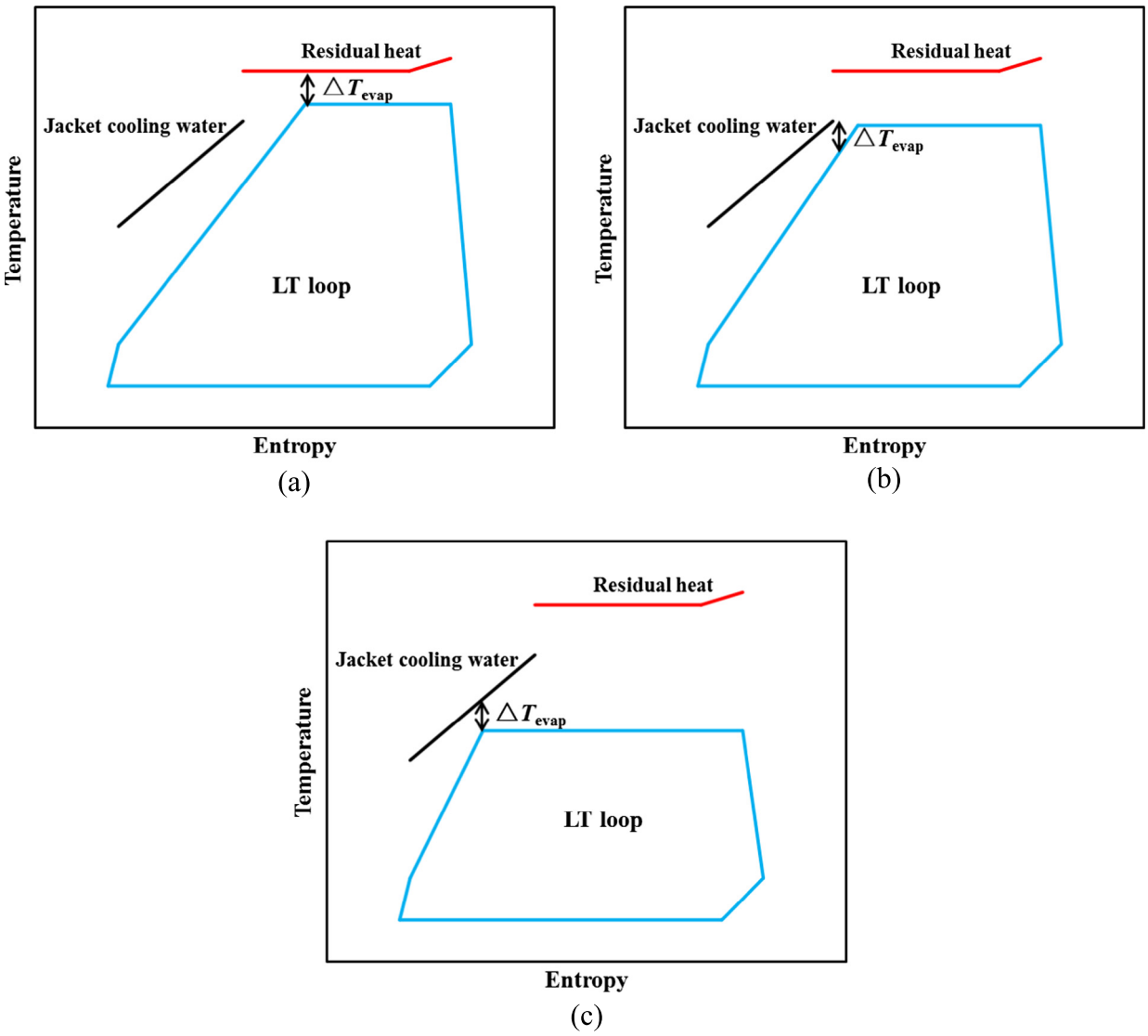

Fig. 6. Three cases of the LT loop with different pinch point locations.

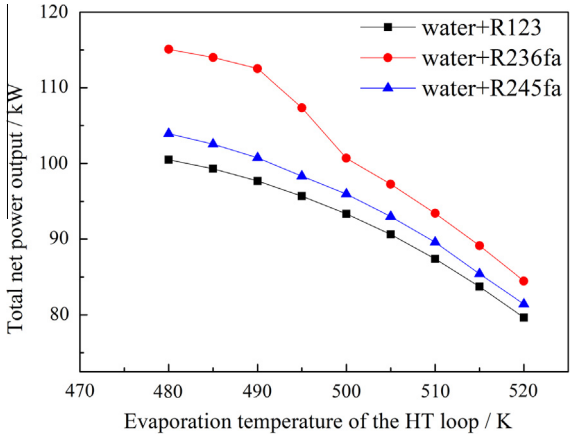

Fig. 7. Total net power output of the dual-loop ORC system.

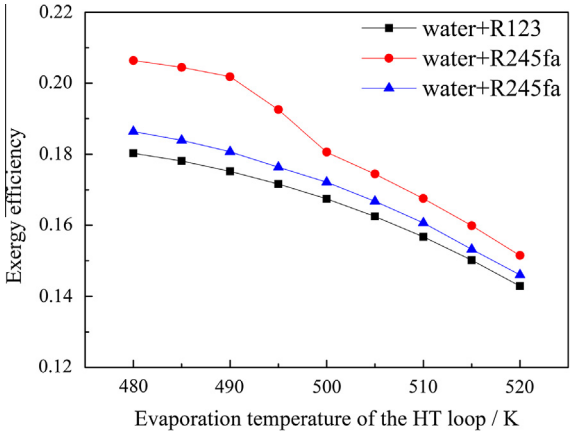

Fig. 8. Exergy efficiency of the dual-loop ORC system.

and the results are shown in Fig. 9. The exergy destruction rates of the pumps in both loops are small, and that of the LT loop is slightly higher due to the higher mass flow rate of the working fluid. The exergy destruction rates of the heat exchangers and the expanders are high, especially for the evaporator of the LT loop, which consists of two heat exchangers for the jacket cooling water

Table 4
Comparison of the ORC system with different working fluids.

	HT loop	LT loop		
	Water	R123	R236fa	R245fa
Evaporation temperature (K)	480.0	347.5	369.0	352.3
Mass flow rate (kg/s)	0.5	2.9	3.3	2.6
Net power output (kW)	54.5	46.0	60.6	49.4
Thermal efficiency (%)	13.1	8.2	10.8	8.8

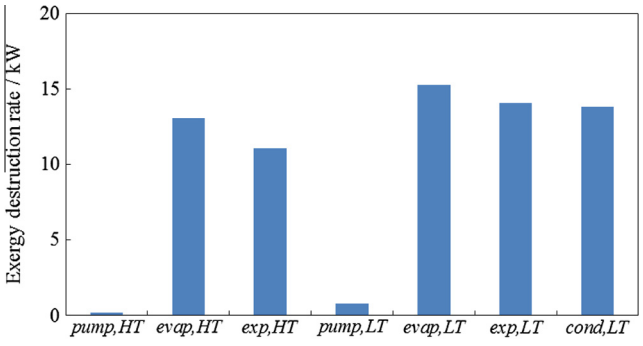

Fig. 9. Exergy destruction rate of each component in the dual-loop ORC system.

and the residual heat of the HT loop. Therefore, optimization of the evaporator of the LT loop is significant to improve the system performance.

5. Conclusions

This paper focuses on waste heat recovery using a dual-loop ORC system on a diesel engine. The high-temperature (HT) loop recovers the waste heat of the engine exhaust gas, while the low-temperature (LT) loop recovers the heat load of the jacket cooling water and the residual heat of the HT loop sequentially. The two loops are coupled via a shared heat exchanger.

Water is selected as the working fluid for the HT loop. The potential of using wet steam expansion, which can be implemented through screw expanders, is investigated in order to achieve a suitable evaporation temperature and a high thermal efficiency. The simulation results show that the HT loop exhibits a better thermal performance for a lower dryness fraction of the wet steam at the inlet of the expander. Wet steam with a dryness fraction of 0.2 is selected, and the maximum net power output for the HT loop is 54.5 kW.

R123, R236fa and R245fa are selected as the working fluid candidates for the LT loop. The influence of the HT loop parameters on the LT loop is evaluated and found to be mainly due to the variable residual heat load of the HT loop. The simulation results reveal that under different operating conditions for the HT loop, the pinch point of the LT loop appears at different locations and results in different evaporation temperatures. For the LT loops with R123 and R245fa as the working fluids, the pinch point only occurs at the jacket cooling water cycle. For the LT loop with R236fa as the working fluid, the pinch point appears at three different locations (i.e., inside of the residual heat cycle, the outlet of the jacket cooling water cycle and inside of the jacket cooling water cycle) and results in different variations of the LT loop thermal parameters. The maximum net power output of the LT loop with R236fa as the working fluid is 60.6 kW when the evaporation temperature equals 369 K, which is the highest net power output that can be reached.

With wet steam (dryness fraction = 0.2) as the working fluid for the HT loop and R236fa for the LT loop, the total net power output reaches 115.1 kW, which leads to an increase of 11.6% on the original power output of the diesel engine. Therefore, the dual-loop ORC system presented in this paper can efficiently recover the waste heat from both the engine exhaust gas and the jacket cooling water. Moreover, the exergy analysis shows that the maximum irreversibility occurs in the evaporator of the LT loop and optimizing this evaporator is an objective for further improving the system performance.

Acknowledgment

This research study was supported by the cooperative scientific research project of energy conversion and emission reduction among China-Europe enterprises (No. SQ2013ZOC200005).

References

[1] Endo T, Kawajiri S, Kojima Y, Yakahashi K, Baba T, Ibaraki S, et al. Study on maximizing exergy in automotive engines. SAE Technical Paper 2007-01-0257; 2007.
[2] Lodwig E. Performance of a 35 HP organic Rankine cycle exhaust gas powered system. SAE Technical Paper 700160; 1970.
[3] Platell OB. Progress of Saab Scania's steam power project. SAE Technical Paper 760344; 1976.
[4] Macián V, Serrano JR, Dolz V, Sánchez J. Methodology to design a bottoming Rankine cycle, as a waste energy recovering system in vehicles. Study in a HDD engine. Appl Energy 2013;104:758–71.
[5] Sprouse III C, Depcik C. Review of organic Rankine cycles for internal combustion engine exhaust waste heat recovery. Appl Therm Eng 2013;51:711–22.
[6] Shu GQ, Li XN, Tian H, Liang XY, Wei HQ, Wang X. Alkanes as working fluids for high-temperature exhaust heat recovery of diesel engine using organic Rankine cycle. Appl Energy 2014;119:204–17.
[7] Yang MH, Yeh RH. Thermodynamic and economic performances optimization of an organic Rankine cycle system utilizing exhaust gas of a large marine diesel engine. Appl Energy 2015;149:1–12.
[8] Teng H, Regner G, Cowland C. Waste heat recovery of heavy-duty diesel engines by organic Rankine cycle Part I: Hybrid energy system of diesel and Rankine engines. SAE Technical Paper 2007-01-0537; 2007.
[9] Teng H, Regner G. Improving fuel economy for HD diesel engines with WHR Rankine cycle driven by EGR cooler heat rejection. SAE Technical Paper 2009-01-2913; 2009.
[10] Bombarda P, Invernizzi CM, Pietra C. Heat recovery from Diesel engines: a thermodynamic comparison between Kalina and ORC cycles. Appl Therm Eng 2010;30:212–9.
[11] Hountalas DT, Mavropoulos GC, Katsanos C, Knecht W. Improvement of bottoming cycle efficiency and heat rejection for HD truck applications by utilization of EGR and CAC heat. Energy Convers Manage 2012;53:19–32.
[12] Srinivasan KK, Mago PJ, Krishnan SR. Analysis of exhaust waste heat recovery from a dual fuel low temperature combustion engine using an organic Rankine cycle. Energy 2010;35:2387–99.
[13] Vaja I, Gambarotta A. Internal combustion engine (ICE) bottoming with organic Rankine cycles (ORCs). Energy 2010;35:1084–93.
[14] Larsen U, Pierobon L, Haglind F, Gabrielii C. Design and optimisation of organic Rankine cycles for waste heat recovery in marine applications using the principles of natural selection. Energy 2013;55:803–12.
[15] Yu GP, Shu GQ, Tian H, Wei HQ, Liu LN. Simulation and thermodynamic analysis of a bottoming organic Rankine cycle (ORC) of diesel engine (DE). Energy 2013;51:281–90.
[16] Song J, Song Y, Gu CW. Thermodynamic analysis and performance optimization of an organic Rankine cycle (ORC) waste heat recovery system for marine diesel engines. Energy 2015;82:976–85.
[17] Shu GQ, Liu LN, Tian H, Wei HQ, Yu GP. Parametric and working fluid analysis of a dual-loop organic Rankine cycle (DORC) used in engine waste heat recovery. Appl Energy 2014;113:1188–98.
[18] Choi BC, Kim YM. Thermodynamic analysis of a dual loop heat recovery system with trilateral cycle applied to exhaust gases of internal combustion engine for propulsion of the 6800 TEU container ship. Energy 2013;58:404–16.
[19] Zhang HG, Wang EH, Fan BY. A performance analysis of a novel system of a dual loop bottoming organic Rankine cycle (ORC) with a light-duty diesel engine. Appl Energy 2013;102:1504–13.
[20] Panesar AS, Morgan RE, Miché NDD, Heikal R. A novel organic Rankine cycle system with improved thermal stability and low global warming fluids. In: MATEC web of conferences, vol. 13. EDP Sciences; 2014. p. 06002.
[21] Smith IK, Stosic N, Mujic E, Kovacevic A. Steam as the working fluid for power recovery from exhaust gases by means of screw expanders. Proc Inst Mech Eng, Part E: J Process Mech Eng 2011;225:117–25.

[22] Qiu GQ, Liu H, Riffat S. Expanders for micro-CHP systems with organic Rankine cycle. Appl Therm Eng 2011;31:3301–7.
[23] Leibowitz H, Smith IK, Stosic N. Cost effective small scale ORC systems for power recovery from low grade heat sources. In: ASME 2006 international mechanical engineering congress and exposition. American Society of Mechanical Engineers; 2006. p.521–7.
[24] Bahadori A. Estimation of combustion flue gas acid dew point during heat recovery and efficiency gain. Appl Therm Eng 2011;31:1457–62.